RSC Advances

ROYAL SOCIETY OF CHEMISTRY

www.rsc.org/advances

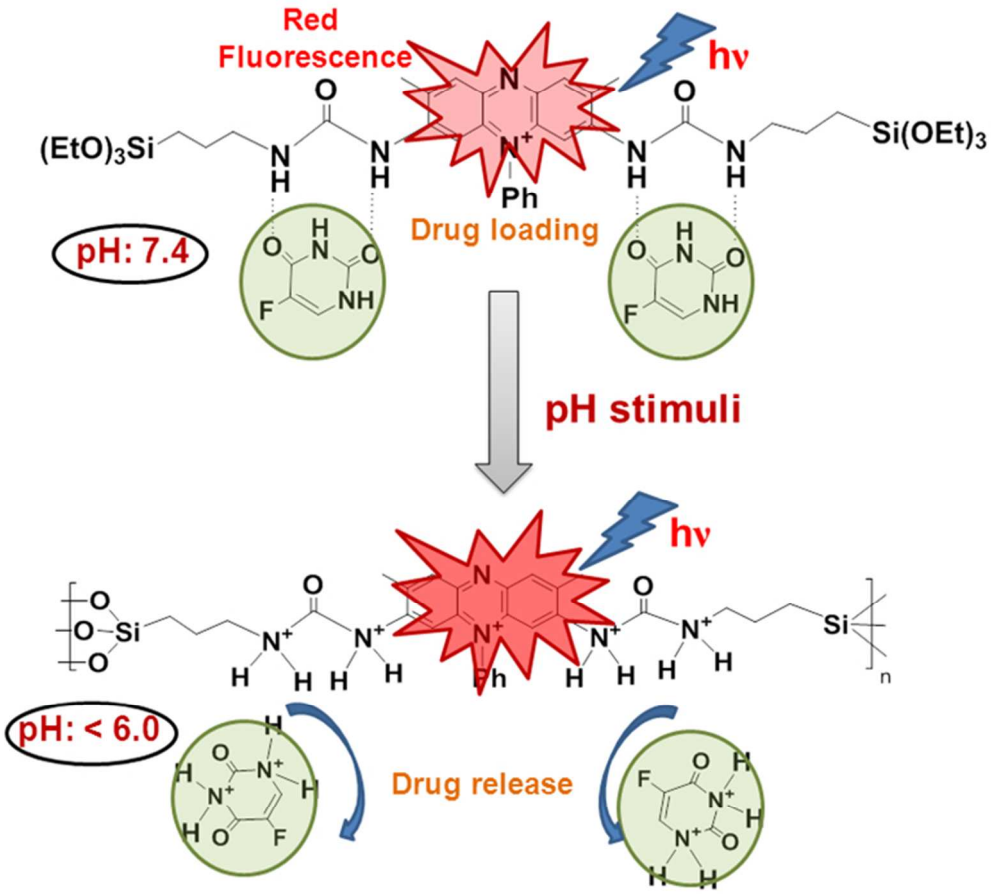

Table of content
Red fluorescent mesoporous organosilica was synthesised for simultaneous diagnosis and therapy, and characterized for anticancer drug delivery behavior.

204x188mm (96 x 96 DPI)

Cite this: DOI: 10.1039/c0xx00000x

www.rsc.org/xxxxxx

ARTICLE TYPE

Red fluorescent hybrid mesoporous organosilicas for simultaneous cell imaging and anticancer drug delivery

Madhappan Santha Moorthy,[a] Hyun-Jin Song,[a] Jae-Ho Bae,[b] Sun-Hee Kim,[b] and Chang-Sik Ha[a]*

A safranin-diurea bridged hybrid mesoporous organosilica (SDU-HMS) was synthesized for simultaneous diagnosis and therapy. This study assessed the impact of integrated functional units on drug loading/release and imaging. The drug delivery efficiency and biocompatibility of the red fluorescent SDU-HMS carrier was evaluated experimentally.

Fluorescent nanoparticles are used in a range of applications involving labeling, tracing and tagging, mainly in biomedical applications.[1,2] Among the range of nanocarriers[3,4] mesoporous silica materials are more suitable delivery vehicles for pharmaceuticals and biomolecules.[5] The high surface area, mesopore volume, high loading efficiency, optical transparency, and biocompatibility of mesoporous silicas[6] make it an ideal candidate as a drug carrier for the loading and controlled release of various drug molecules.[7,8] The development of mesosporous organosilica hybrids for theranostic applications are still in demond.[9] Owing to the luminescent framework properties, the fluorescent organosilica hybrid materials are considered to be a suitable system for fluorescent-based drug carriers desirable for biomedical imaging, diagnostic, and traceable site-specific therapy. Stimuli-responsive drug delivery strategy is considered a promising technique for safe, controlled and site specific target delivery to avoid undesirable side-effects to the normal tissues.[10] Among the various stimuli, pH-responsive based controlled delivery is considered a simple and efficient method because the specific pH differs according to the tissues and cellular components in human and living bodies.[11-12] To administer the drug molecules to the specific target tissues, pH responsive functional molecules,[13] nanoparticles[14] and peptides[15] are generally introduced as gate keeper for controlled release of encapsulated cargos in responding to internal/external stimuli. Unfortunately, these approaches have some drawbacks, such as multi-step modification process, steric hindrance, and weak physical absorption of the cargo. The release efficiency of the encapsulated cargo could be controlled with respect to the differences in pH between the tumor and normal tissues. Such systems could prevent premature leakage of the payload under physiological pH conditions and have higher release efficiency with enhanced release behavior under decreased pH conditions.

This paper reports the synthesis of a novel mesoporous organosilica nanocarrier with drug interacting ligand sites that can hold the loaded drugs by the strong complementary H-bonding interactions and release them to the specific target sites with respect to the pH of the release medium. The derivatized diurea groups and the integrated safranin fluorophore into the silica framework allow the material to be utilised as a pH-responsive red fluorescent drug carrier. In addition, the prepared safranin-diurea (SDU) bridged hybrid mesoporous organosilicas (SDU-HMS) showed good biocompatibility. An excellent red fluorescent was observed in the cells under UV-light owing to the presence of integrated safranin units in the mateials.

Scheme 1 shows the synthesis of SDU-HMS material. Fig. S1 (ESI†) shows the powder X-ray diffraction (XRD) pattern of SDU-HMS sample. The XRD peak at 2.45 2θ (d = 3.6 nm) and a weak peak at 4.08 2θ (d = 2.1 nm) have been observed that indicates the formation of well-ordered mesostructural arrangement of the material. Fig. S2 (ESI†) shows N_2 sorption isotherm of the SDU-HMS material. As shown in Fig. S2 (ESI†), the SDU-HMS sample exhibited type IV isotherm curve with H1 hysteresis suggesting the formation of well-ordered mesoporous materials. The Brunauer-Emmet-Teller (BET) surface area was determined to be 685 m^2/g, and the pore volume and mean mesopore diameter was calculated to be 0.24 cm^3/g^{-1} and 3.2 nm (Table S1, ESI†). Fig. S3 (ESI†) shows the Fourier transform infrared (FTIR) spectrum of the SDU-HMS sample. The typical bands at 1543 cm^{-1}, 1482 cm^{-1}, 1652 cm^{-1}, 1382 cm^{-1} and 782 cm^{-1} respectively, indicating the existence of functional safranin

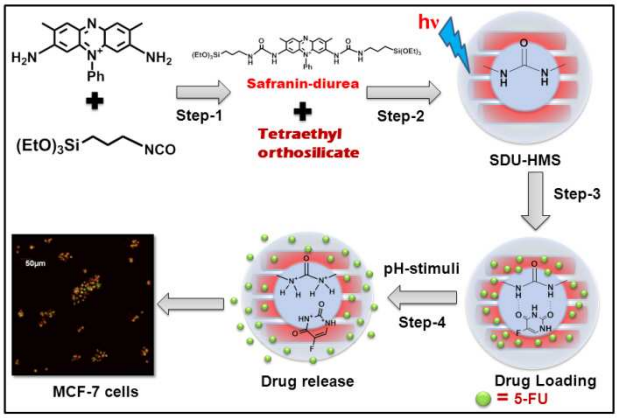

Scheme 1. Synthesis of the SDU precursor (Step-1) and preparation of the functionalised SDU-HMS materials (Step-2).

[a]*Department of Polymer Science and Engineering, Pusan National University, Busan 609-735, Korea. E-mail: csha@pnu.edu*
[b]*Department of Biochemistry, School of Medicine, Pusan National University, Yangsan Hospital, Yangsan 626-870, Korea*
† Electronic supplementary information (ESI) available: Experimental details and supporting figures.

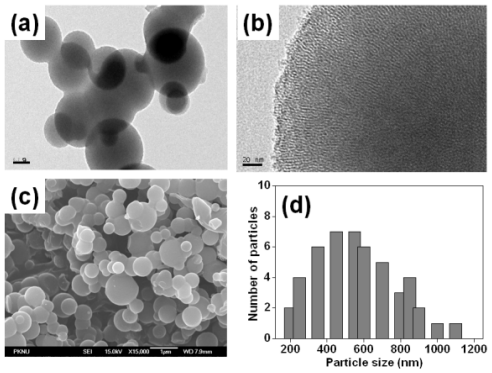

Fig. 1 (a,b) Transmission electron microscopy (TEM), (c) scanning electron microscopy (SEM) images and (d) particle size distributions of the SDU-HMS material.

fluorophores in the materials pore walls.[16] The intense stretching peaks at 1124 cm^{-1} and 963 cm^{-1} revealed the presence of Si-O-Si and Si-OH bonds of the silica network. In addition, the peaks at 2852 cm^{-1} and 2918 cm^{-1} for the alkyl C-H stretching vibrations can confirm the presence of covalently-integrated fluorescent moieties in the mesopore walls. Fig. 1(a,b) presents TEM images of the SDU-HMS, which evidenced the formation of mesopore channels with a mean pore size of approximately 3 nm. The SEM image of the SDU-HMS materials revealed the formation of spherical particles with a mean particle size of ~500-600 nm and almost uniform particle size with slight aggregation (Fig. 1(c)). The mean particle size of the SDU-HMS sample was measured by dynamic light scattering (DLS). The DLS data revealed the particle size is in the range, 200 nm-1.1 μm (Fig. 1(d)). Majority of the particles size belong to 200-800 nm. Generally, the large particle sizes are in some cases not reliable for cellular uptake process for the cells with small sizes. In contrary, the particle size is about ~ 1 μm may be suitable for the cells with comparatively large sizes such as MCF-7 and HeLa cells.[17,18] Therefore, we assume that the SDU-HMS particles of the sizes in the range 200-800 nm can be efficiently internalized by MCF-7 cells plausibly due to the formation of protein corona on the SDU-HMS particles.[19] More systematic investigations may be necessary, however, after separating particles, to reveal the size effect on the cellular uptake, with referring to literatures including Lu et al.'s report.[20]

The ^{13}C cross polarized magic angle spectrum (CP MAS) (Fig. S4 (ESI†)) exhibited the resonance signals in the range, 0-30 ppm indicating the presence of alkyl carbon atoms, Si-CH_2, -CH_2 and CH_2-O confirming the presence of bridged organosilane groups. In addition, the carbon resonance signals at 43.5 ppm and 59.8 ppm were assigned to the aromatic -CH_2 and C-N^+-C carbon atoms, respectively, indicating the presence of functional safranin fluorophore that was integrated covalently in the pore walls.[21] In addition, the resonance signals at 120 ppm and 160 ppm, and a broad weak peak at 209 ppm were assigned to the C-N, C=C and C=O carbon atoms, which further confirmed the presence of a covalently integrated organosilane precursor in the pore walls of the SDU-HMS material.[22] Thermogravimetric analysis (TGA) profile (Fig. S5, ESI†) showed that the initial weight loss of approximately 2 wt% at 100 ºC was due to the evaporation of the physisorbed water. Major weight loss occurred at temperature between 101 to 650 ºC due mainly to decomposition of the integrated SDU precursor in the SDU-HMS pore walls. The elemental analysis used to determine the amount of SDU functional moieties into the SDU-HMS material was 0.023 mol/g. We also checked the stability of the SDU-HMS at different time and pH conditions and we found that no considerable change of fluorescence intensity was observed even after 48 h in pH 7 (Fig. S6(a), ESI†). The fluorescence behavior was almost same at different pHs (4 to 8) (Fig. S6(b), ESI†). Therefore, the stable fluorescence behavior of the SDU-HMS drug carriers under acidic pH conditions can facilitate the prolonged *in vivo* tracking of these drug delivery vehicles. The combined dual fluorescent and pH-responsive release behavior of the SDU-HMS is considered to be more beneficial in *in vivo* imaging cancer therapy over the previously reported our pH-responsive drug carrier.[23]

The *in vitro* drug release profiles (Fig. 2) of the SDU-HMS nanocarrier showed a pH-responsive drug release behavior, and the drug release was increased significantly with decreasing pH from pH 7.4 to 4. The drug loading and release phenomena could be explained based on the interactions between the drug molecules 5-Fluorouracil (5-FU) with the -NH-CO-NH- part of the diurea ligands that exist in the pore walls of the SDU-HMS sample. Complementary multiple H-bonding/electrostatic interactions were expected between the drug molecules and the diurea ligand sites, which play a critical role in the drug storage and pH-responsive release behavior owing to their appropriate host-guest binding orientations.[23] High-performance liquid chromatography(HPLC)-mass spectrometer(MS) can also be applicable to determine the ligand-drug interactions.[24] However, in this work, the interactions of 5-FU with diurea moieties were confirmed based on the change of fluorescence intensities before and after drug loading (Fig. S7, ESI†). The drug release profiles reveal that about 18 % to 87 % of the 5-FU release was achieved by adjusting the pH from 7.4 to 4 (Fig. 2). In particular, 5-FU release was very slow at about 18 % under physiological pH conditions. In contrast, at lower pHs, the release behavior was increased to ~ 42 %, 54 % and 87 % at pH 6, 5.6 and 4, respectively, at 24 h. This is because the dissociation of the existing H-bonding interactions caused electrostatic repulsion between the protonated part of the diurea groups and the 5-FU molecules, as shown in Scheme S1 (ESI†). Under acidic pH conditions, the amine groups of the diurea moieties become positive charge due to protonation, and strong electrostatic repulsion would be expected between the drug molecules and the protonated ligand centers with respect to the pH of the release medium. Therefore, the SDU-HMS is desirable for anticancer drug delivery applications.

The 3-(4,5-dimethylthiazol-2-yl)-2,5-diphenyltetrazolium bromide (MTT) assay was performed to evaluate the cytotoxicity of the SDU-HMS at pH 6. As shown in Fig. S8 (ESI†), the blank SDU-HMS carrier (green band) showed no considerable cytotoxicity to MCF-7 cells at the sample concentrations tested (10, 25, 50 and 100 μg mL^{-1}) after a 24 h incubation period. It reveals that the SDU-HMS was non-toxic and biocompatible. On the other hand, the 5-FU loaded SDU-HMS samples at various concentrations (10, 25, 50 and 100 μg mL^{-1}) exhibited concentration dependent cytotoxicity of approximately 20-82 %

(pink band) under acidic pH (pH 6). The concentration dependant

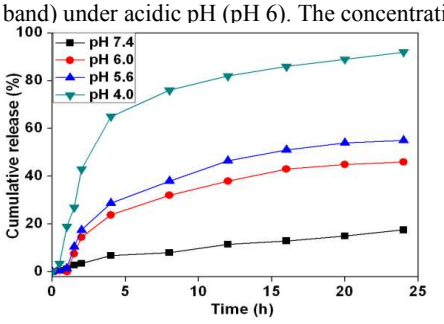

Fig. 2 Drug release profiles of 5-FU from the SDU-HMS carrier in a PBS buffer at pH 7.4, 6, 5.6 and 4 at 37 ° C.

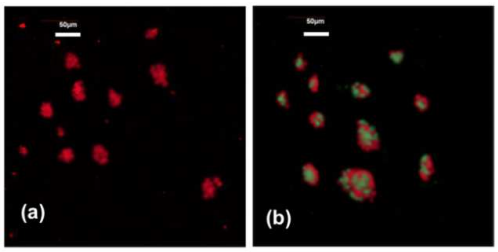

Fig. 3 Fluorescence confocal microscopy images of MCF-7 cells after 6 h incubation. CLSM images of MCF-7 cells with (a) pure SDU-HMS particles and (b) fluorescein (FITC)-labelled SDU-HMS at pH 6. Scale bar = 50 μm.

cytotoxicity might be induced due to the release of the loaded 5-FU. Therefore, the higher concentration of drug carriers into the cells was responsible for releasing higher amounts of the 5-FU molecules into the cells, and inducing increased cancer cell death (Fig. S8, ESI†). The simultaneous imaging and drug delivery is beneficial for potential nanocarriers. The red fluorescence signal would be very useful for tracking the location of the carrier particles into the living body. The confocal images (Fig. 3(a) showed intense red signals within the cells under UV-light, indicating the presence of internalised red fluorescent SDU-HMS nanocarriers into the cells. In addition, the drug loading/release efficiency of the SDU-HMS nanocarrier with respect to pH of the cancer cells was evaluated using MCF-7 cells as the model target cellular sites. For this purpose, fluorescein (FITC) labelled 5-FU was chosen as a model cargo. As shown in (Fig. 3(b)) the red and green fluorescence in the human breast cancer (MCF-7) cells indicate the internalised SDU-HMS carriers and released FITC-labelled 5-FU molecules under acidic conditions. The confocal image indicating the internalised SDU-HMS nanoparticles and the efficient release of the FITC labelled 5-FU molecules under acidic pH conditions. Owing to the red-fluorescence behavior, the SDU-HMS nanocarrier could be used as a red-fluorescent-based tracer for bioimaging and acts as the efficient drug carrier system for loading and pH-responsive release of anticancer agents to the target cancer sites. We have tested the uptake of particles at different concentrations such as 1 μg/mL, 10 μg/mL and 50 μg/mL, and we observed that the fluorescence intensity of the internalized SDU-HMS particles at 10 μg/mL was about 40 % lower than that at 50 μg/mL. On the other hand, the fluorescence intensity was low when the cells were incubated with 1 μg/mL. This suggests the efficient uptake of the SDU-HMS particles by MCF-7 cells (Fig. S9, ESI†).

In summary, a red fluorescent SDU-HMS nanocarrier was synthesised by co-condensation method. The *in vitro* drug release study showed that the SDU-HMS material possesses the loading/release ability of anticancer agents. The MTT assay showed that the SDU-HMS is biocompatible and potentially useful for cancer treatment. In addition, the SDU-HMS nanocarrier exhibited strong red fluorescence within the MCF-7 cells upon irradiation with UV-light (365 nm), suggesting that the SDU-HMS nanocarriers might be useful for *in vivo* cell imaging. These experimental results proved that the SDU-HMS nanocarrier would be desirable for the red fluorescence based *in vitro* tracking and pH-responsive anticancer drug release in cancer therapy. It should be noted, however, forming the protein corona may significantly change the cellular uptake behavior of SDU-HMS. As a proof of concept, we demonstrated here a new biocompatible and pH sensitive material for drug delivery applications. Therefore, we will design methods to manufacture corona-free nanomaterials in our future work.

We thank the National Research Foundation of Korea (NRF) Grant funded by the Ministry of Science, ICT & Future Planning, Korea; Pioneer Research Center Program (2010-0019308/2010-0019482); NRF-RFBR Joint Research Program (2013K2A1A7076267); Brain Korea 21 Plus Program (21A2013800002).

References

1. B.S. Edwards, T. Oprea, E.R. Prossnitz, L.A. Sklar, *Curr. Opin. Chem. Biol*. 2004, **8**, 8392.
2. J.L. Vivero-Escoto, I.I. Slowing, B.G. Trewyn, V.S.-Y. Lin, *Small*. 2010, **6**, 1952.
3. X. Gao, Y. Cui, R.M. Levinson, L.W.K. Chung, S. Nie, *Nat. Biotechnol*, 2004, **22**, 969.
4. K. Miyata, N. Nishiyama, K. Kataoka, *Chem. Soc. Rev*. 2012, **41**, 2562.
5. P. Yang, S. Gai, J. Lin, *Chem. Soc. Rev.* 2012, **41**, 3679.
6. C.T. Kresge, M.E. Leonowich, W.J. Roth, J.C. Vartuli, J.S. Beck, *Nature.* 1992, **359**, 710.
7. M. Vallet-Regi, M. Colilla, B. Gonzalez, *Chem. Soc. Rev*. 2011, **40**, 596.
8. A. Stein, B.J. Melde, R.C. Schroden, *Adv. Mater*. 2000, **12**, 1403.
9. D. Lu, J. Lei, L. Wang, J. Zhang, *J. Am. Chem. Soc.* 2012, **134**, 8746.
10. F. Kohori, K. Sakai, T. Aoyagi, M. Yokoyama, Y. Sakurai, T. Okano, *J. Controlled Release,* 1988, **55**, 87.
11. Y. Qui, K. Park, *Adv. Drug Delivery Res*. 2001, **53**, 321.
12. E.S. Lee, K.T. Ch, D. Kim, Y.S. Yown, Y.H. Bae, *J. Controlled Release*, 2007, **123**, 19.
13. Z. Luo, K.Y. Cai, Y. Hu, L. Zhao, P. Liu, L. Duan, W.H. Yang, *Angew. Chem. Int. Ed*. 2011, **50**, 640.
14. H.P. Rim, K.H. Min, H.J. Lee, S.Y. Jeong, S.C. Lee, *Angew. Chem. Int. Ed.* 2011, **50**, 8853.
15. F. Porta, G.E.M. Lamers, J.I. Zink, A. Kros, *Phys. Chem. Chem. Phys*. 2011, **13**, 9982.
16. X. Peng, J. Du, J. Fan, J. Wang, Y. Wu, J. Zhao, S. Sun, T. Xu, *J. Am. Chem. Soc*. 2007, **129**, 1500.
17. V. Vergaro, E. Abdullayev, Y.M. Lvov, A. Zeitoun, R. Cingolani, R. Rinaldi and S. Leporatti, *Biomol.* 2010, **11**, 820.
18 Z. Mao, X. Zhou and C. Gao, *Biomater. Sci*., 2013, **1**, 896.
19. C.D. Walkey, W.C. Chan, *Chem. Soc. Rev*. 2012, **41**, 2780.
20. F. Lu, S.-H. Wu, Y. Hung and C.-Y. Mou, *Small*, 2009, **5**, 1408.
21. C. Coll, A. Bernordos, R. Martinez-Menaz, F. Sancenon, *Acc. Chem. Res*. 2013, **46**, 339.
22. a) R.J.P. Corriu, *Angew. Chem. Int. Ed*. 2000, **39**, 1376; b) R. Dong, B. Zhu, D. Yun, X. Zhu, *Angew. Chem. Int. Ed*. 2012, **51**, 11633.
23. M.S. Moorthy, J.-H. Bae, M.-J. Kim, S.-H. Kim, C.-S. Ha, *Part. Part. Syst. Charact.* 2013, **30**, 1044.
24. a) B. Yan, Y. Jeong, L. A. Mercante, G.Y. Tonga, C. Kim, Z.-J. Zhu, R.W. Vachet and V.M. Rotello, *Nanoscale*, 2013, **5**, 5063; b) H. Zhou, X. Li, A. Lemoff, B. Zhang and B. Yan, *Analyst*, 2010, **135**, 1210.